COBEM 2023 27TH INTERNATIONAL CONGRESS OF MECHANICAL ENGENEERING

ABCM Brazilian Society of Mechanical Sciences and Engineering
27th ABCM International Congress of Mechanical Engineering
December 04-08, 2023, Florianópolis-SC, Brazil

COB-2023-2259
STUDY OF APPROXIMATION MANEUVERS WITH CLOSED-LOOP CONTROL FOR A SPACECRAFT OVER ASTEROIDS

Luan Henrique Glasser
Evandro Marconi Rocco
Instituto Nacional de Pesquisas Espaciais, Avenida dos Astronautas, 1758 - Jardim da Granja, São José dos Campos - SP, 12227-010
luan.glasser@gmail.com, evandro.rocco@inpe.br

Marcelo Lisbôa Mota
Instituto Federal de Educação, Ciência e Tecnologia de São Paulo, Avenida Thereza Ana Cecon Breda, 1896 - Vila São Pedro, Hortolândia - SP, 13183-250
prof.mlmota@ifsp.edu.br

Abstract. *In the last forty years, asteroid exploration came into focus of nations as United States, China, Japan and also to European Union. An evidence of that is the number of asteroid missions that happened during this period, among which the Hayabusa and the Osiris-REX can be found. In this time, the complexity of the missions have evolved from distant flybys, to sample-return, to asteroid deflection missions, so that, consequently, have also evolved sensors, actuators, overall equipment, instruments and, by extension, the spacecraft. Asteroid exploration is one of the space science, engineering and technology frontiers. Mastering this knowledge and ability is a key for the past, in order to understand Solar System formation and, maybe, the origin of life, but also for the future, making space more accessible for humankind. The challenge imposed to a spacecraft for it to move in an interplanetary flight, approach an asteroid and land is central in this discussion. The objective of this work was to study procedures for approaching a spacecraft to the asteroids (8567) 1996 HW1 and (1580) Betulia, in order to compute maneuvers with less velocity increment usage, to find landing conducive conditions and to simulate the complete maneuvers of approximation and landing. The Spacecraft Trajectory Simulator is a simulation environment dedicated to study spacecraft dynamics and trajectories, capable of performing guidance and control, and it was the main tool used to realize this work. As research results, this work has produced two maps, one for each asteroid, of landing conducive conditions. The maps could be used in mission analysis, to select landing conducive conditions and as input for mission design. This work has also demonstrated the usage procedure of those maps, successfully computed the consumption of velocity increments for different maneuvers and simulated complete maneuvers of approximation and landing.*
Keywords: *spacecraft dynamics, PID controller, orbital maneuvers, asteroids, landing*

1. INTRODUCTION

In the last 40 years, humankind has seen intense and growing activities regarding asteroid exploration, as Clark *et al.* (2018) and, among others, Veverka *et al.* (1994), Mitchell (2000), Hashimoto *et al.* (2010), Beshore *et al.* (2015), Taylor *et al.* (2017), Mingtao and Kaiduo (2022), and Daly *et al.* (2023) made clear. From basic flybys to sample return missions, from sample return missions to asteroid deflection, the theme has been growing in importance, as did the expertise regarding it, and the technological capabilities of the spacecrafts. Deep space exploration is important to make space more accessible, and also to allow better understanding of Solar System formation and, maybe, even the origin of life. Mastering this knowledge and ability is vital for future deep space exploration and planetary defense.

This research is an attempt to contribute to this scientific endeavor and moves along with the global increasing interest in deep space exploration. The objectives of this work were to: (1) study maneuvers for approaching a spacecraft to the asteroids (8567) 1996 HW1 and (1580) Betulia, to understand the velocity increment usage; (2) find landing conducive conditions (LCC); and (3) to simulate the complete maneuvers of approximation and landing, showing the application of the LCC. The core tool used in this work was Spacecraft Trajectory Simulator (STRS), developed by Rocco (2008). The STRS is one of the simulation tools of the Modeling and Simulation Laboratory of Dynamics and Control in Closed-Loop of the Orbit and Attitude of Space Vehicles (Lab MSDC Orbit & Attitude), at the Space Mechanics and Control Division (DIMEC) of the *Instituto Nacional de Pesquisas Espaciais* (INPE, National Institute of Spatial Research). The asteroids gravitational potential were modeled by Mota (2017), with the gravitational potential expansion in convergent series method.

The next sections will present the fundamental theory needed for this work, followed by the methodology. Then, the results will be presented, firstly regarding the asteroid (8567) 1996 HW1, then for the asteroid (1580) Betulia. Conclusions and references can be found further.

2. FUNDAMENTAL THEORY

2.1 Dynamics

Two coordinate systems were used to compute and show the trajectories: Body-Center Inertial (BCI) and Body-Center Body-Fixed (BCBF). Both of the coordinate systems are centered in the asteroids mass centers, but BCI has an arbitrary inertial orientation, while BCBF has its axes fixed in the asteroid body frame, in the directions of the principal axes. I the beginning of any simulation, it was considered that BCI and BCBF were aligned. Also, during the simulation, BCI and BCBF z-axes were always aligned.

According to Mota (2017), the dynamic model of the system is

$$\ddot{\mathbf{r}} = \nabla U \tag{1}$$

where $\ddot{\mathbf{r}}$ is the acceleration of the vehicle and U is the gravitational potential.

Mota (2017) developed a method to model the gravitational potential in a convergent series expansion, for a homogeneous body discretized in tetrahedral elements, which was applied to model the asteroids gravitational fields studied in this work. This method[1] leads to

$$U = G\frac{m}{\mathcal{V}}\sum_{i=1}^{N}\iiint_{Q} P_i \frac{R^i r^i}{r^{2i+1}} d\mathcal{V} + \epsilon \tag{2}$$

where G is the universal gravity constant, m is the asteroid mass, $\mathcal{V}$ is the volume, Q is any of the tetrahedral elements that compose the asteroid discretization and over which the integrals are calculated, P_i are Legendre polynomials. The module of the distance of a mass element inside the asteroid, with respect to the asteroid mass center, is R, and r is the module of the position vector of a particle with respect to the asteroid mass.

Applying this method leads the expression

$$U = U_0 + \sum_{i=1}^{N} U_i + \epsilon, \tag{3}$$

where U_0 represents the keplerian potential, $\sum_{i=1}^{N} U_i$ is the perturbation potential expanded to order N and ϵ is the truncation error. In this work, N = 6. The asteroid shape discretization models, that were generated through radar observations, and to which this method was applied, can be found in Frieger (2021).

2.2 Calculating maneuvers with the solution of the Lambert's problem

Battin (1999) explains the problem to connect two position vectors $\mathbf{r}_1$ and $\mathbf{r}_2$, in two different orbits, angled from each other by $\Delta\theta$, with an orbit, is called Lambert's problem. The first person recorded to solve it was Carl Friedrich Gauss, in 1801, and his solution was used to predict Ceres position in the same year. The Lambert's problem solution returns two velocity increments, $\Delta\mathbf{v}_1$ and $\Delta\mathbf{v}_2$, which must be applied in the beginning and in the end of a maneuver. Figure 1 describes the problem.

According to Rocco (2015), a procedure to solve this problem is as it follows. The goal is to find $\mathbf{v}_1$ and $\mathbf{v}_2$:

$$\mathbf{v}_1 = \frac{\mathbf{r}_2 - f(z)\mathbf{r}_1}{g(z)},\ \mathbf{v}_2 = \frac{\dot{g}(z)\mathbf{r}_2 - \mathbf{r}_1}{g(z)} \tag{4}$$

where $f(z)$ and $g(z)$ are universal variables. To determine these function values, calculate:

$$A' = sign(\pi - \Delta\theta)\sqrt{|\mathbf{r}_1||\mathbf{r}_2|(1+\cos\Delta\theta)},\ \Delta\theta = \arccos\left(\frac{\mathbf{r}_1.\mathbf{r}_2}{|\mathbf{r}_1||\mathbf{r}_2|}\right). \tag{5}$$

where A' in an auxiliary variable.

Then, evaluate the movement direction: if $sign(\pi - \Delta\theta) = -1 \rightarrow \Delta\theta > \pi$ and the trajectory to be performed is the long one; otherwise, it is the short one.

[1] The full description of the method can be found on Mota (2017), as asteroid gravitational potential models for which the method was applied.

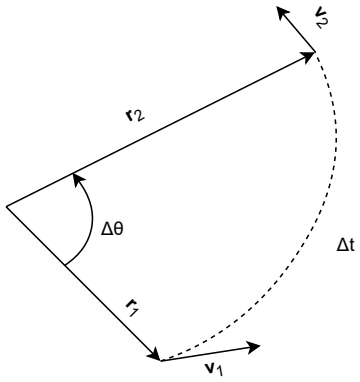

Figure 1. Schematics to the Lambert's problem.

Then, solve:

$$F(z) = x^3(z)S(z) + A'\sqrt{y(z)} - t_m\sqrt{\mu} = 0 \tag{6}$$

where t_m is the maneuver time and:

$$S(z) = \frac{\sqrt{z} - \sin\sqrt{z}}{\sqrt{z^3}},\ C(z) = \frac{1-\cos\sqrt{z}}{z},\ y(z) = |\mathbf{r}_1| + |\mathbf{r}_2| - A'\frac{1-zS(z)}{\sqrt{C(z)}},\ x(z) = \sqrt{\frac{y(z)}{C(z)}}. \tag{7}$$

where $z \in R : 0 \leq z \leq (2\pi)^2$. Following that, the function $F(z)$ can be numerically solved by scanning the interval in which z is allowed to vary, until a solution converges. Then, $f(z)$ and $g(z)$ can be calculated:

$$f(z) = 1 - \frac{y(z)}{|\mathbf{r}_1|},\ g(z) = A\sqrt{\frac{y(z)}{\mu}},\ \dot{g}(z) = 1 - \frac{y(z)}{|\mathbf{r}_2|}. \tag{8}$$

And, finally, the maneuver velocity increments can be obtained by:

$$\Delta\mathbf{v}_1 = \mathbf{v}_1 - \mathbf{v}_0,\ \Delta\mathbf{v}_2 = \mathbf{v}_f - \mathbf{v}_2, \tag{9}$$

in which $\mathbf{v}_0$ and $\mathbf{v}_f$ are the velocities of the initial and final orbits. This method was used to calculate all the maneuvers presented in this work.

2.3 Controlling the spacecraft trajectory and perturbations

According to Ogata (1997), to control a system is to impose the system a desired behavior. There is a huge amount of methods to achieve this, but a simple and effective one is the use of a PID controller, which stands for Proportional, Integral and Derivative controller:

$$\mathbf{u} = K_p\mathbf{e} + K_i\int_0^t \mathbf{e}dt + K_d\frac{d\mathbf{e}}{dt}, \tag{10}$$

where $\mathbf{u}$ is the control signal, $\mathbf{e}$ is the error, K_p is the proportional gain, K_i is the integral gain, and K_d is the derivative gain. The proportional term amplifies the error signal, the integral term integrates the error signal, and the derivative term derives the error signal. The usage of this control technique will be explained in the next section.

3. METHODOLOGY

This section will present the methodology. Fist, tool, concepts and ideas which the methodology used will be explained. Then the research method, which used these concepts, will be described.

3.1 Tool, concepts and ideas used in the research method

3.1.1 Spacecraft Trajectory Simulator

The STRS is a simulation environment developed on MATLAB/Simulink by Rocco (2008), Rocco (2010), Rocco (2013b) and Rocco (2013a). The objective of the simulator is to provide means for simulating closed-loop controlled spacecraft trajectories. Several features and capabilities are included in STRS. It embeds orbital mechanics, gravitational models for a diverse scope of spatial bodies, control systems, guidance, and many other features, which are organized into the architecture shown in Figure 2 (left side). STRS was the main tool used in this research.

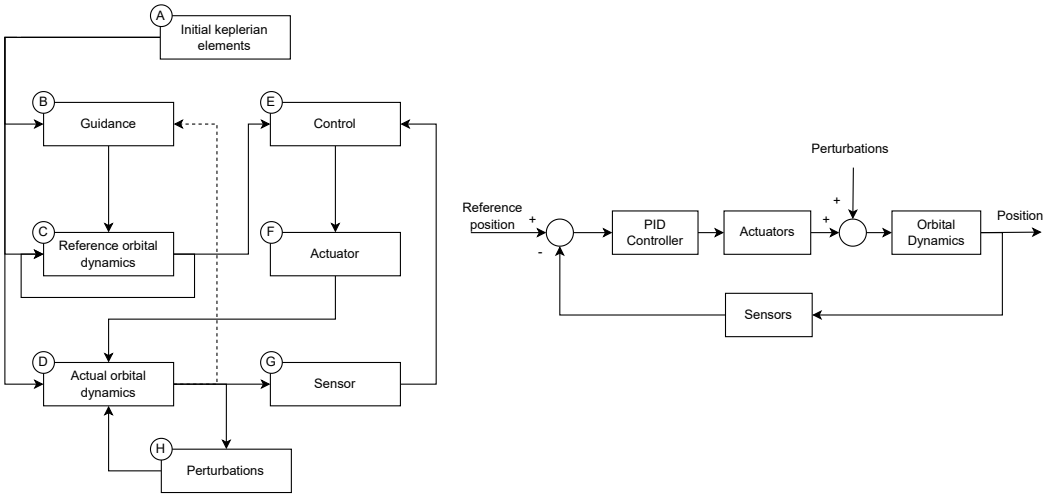

Figure 2. Left side: STRS architecture. Right side: implementation of the control system inside STRS.

3.1.2 Trajectory control

Figure 2 (right side) shows the control system implementation in a block diagram, which is embedded in the STRS. The control system can be turned on and off at will. The control variable is the vehicle position. For the actuators it was considered modulated continuous 2 N thrusters and the controller gains used in this research were: K_p = 0,050, K_i = 0,001, and K_d = 0,025. These gains were selected via a test-adjust process, to be sufficient to provide a trajectory control. It was not in the scope of this work to develop a control gains performance study, which will be left for future work.

3.1.3 Calculating altitude and velocity with respect to the surface

The asteroid shape models were taken from Frieger (2021), which discretize the bodies surfaces into triangles from radar observations. The STRS reads this model and calculates the vectorial positions of the barycenters of each of those triangles. At each simulation step, an algorithm checks the distance from the spacecraft to all barycenters and selects the closest barycenter. The altitude of the spacecraft in this simulation step is the distance from vehicle to the closest barycenter of the surface discretization triangle. Velocity with respect to the surface is calculated by computing the difference from the actual barycenter to the previous one, divided to the simulation time step.

3.1.4 Orbit definitions

In order to plan the maneuvers and categorize the results, it was needed useful definitions of orbital regions around the asteroid. It was adopted the terminology: high, middle, low and terminal orbits, which are defined by Figure 3, based on the sphere of influence radius (SIR), as calculated by Fernandes and de Paula Santos Zanardi (2018), and the radius of the circumscribing sphere R_c.

3.1.5 Approximation maneuvers

The maneuvers studied in this research were made in two phases of approximation, an initial approximation from a high to a low orbit; and a terminal approximation from a low to a terminal orbit. The orbits were always equatorial ones. The vehicle was modeled as a point of mass. Initial approximation begins in a high circular orbit, with a true anomaly of about zero degree and ends in a low circular orbit with a true anomaly of about 180 degrees. Terminal approximation begins in a low circular orbit, when the true anomaly is approximately 180 degrees, and ends in a circular terminal orbit, when the true anomaly is approximately 360 degrees. The velocity increments were calculated by solving the Lambert's

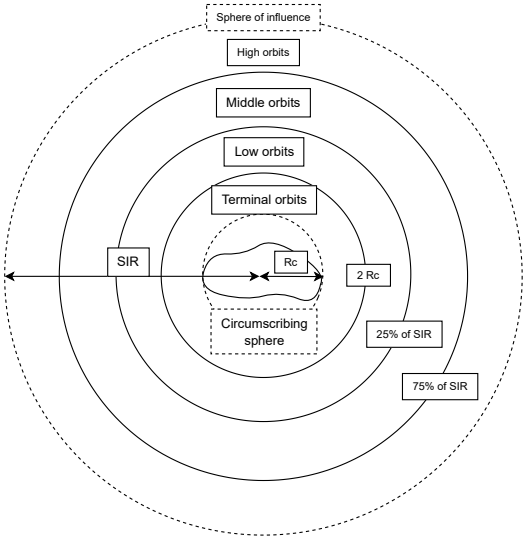

Figure 3. Orbit definitions.

problem for each maneuver phase. All the approximation maneuvers were trajectory controlled. The performance of the approximation maneuvers was evaluated in terms of total velocity increments.

3.1.6 Landing conducive conditions

It was observed that there were some conditions, in terms of radial and angular position with respect to the asteroid, on equatorial orbits from which the vehicle would land in less than 50.000 s, only by influence of the gravitational perturbation. These conditions were defined as landing conducive conditions (which are stood by LCC, as previously mentioned). For each asteroid, to map the LCC, a set of 372 simulations was configured and executed. Each simulation baseline was as the following: BCI and BCBF coordinates aligned in the initial time; initial circular orbits; radial position and relative angular position to the asteroid were varied on each simulation, in order to get a map of points around the asteroid that were or were not LCC.

3.1.7 Approximation maneuvers and landing from an LCC procedure

Complete approximation maneuvers were simulated to bring a spacecraft from a high to a terminal orbit, to reach an LCC and from there land. These simulations showed use cases for using the LCC maps combined with approximation maneuvers. The procedure for using the LCC map in this work, in order to achieve this result, was the following:

1. calculate the approximation maneuver to bring the spacecraft to a terminal obit which contains an LCC;
2. configure a simulation with the calculated maneuver, controlling the trajectory, so the vehicle can stay as long as possible hovering in a terminal orbit;
3. execute the simulation and plot the maneuver results;
4. using the LCC map, identify in the simulation results what orbital position is an LCC and get the simulation time where the condition is achieved;
5. evaluate if in this time the orbit is circular, if not, calculate the necessary velocity increment to make the orbit circular;
6. configure another simulation such as the previous, but, now, when the vehicle reaches the selected LCC, turn off the trajectory control and apply the velocity increment to make the orbit circular;
7. execute the simulation;
8. evaluate the landing results.

3.2 Research method

Using the above concepts and ideas, the research method, for each asteroid, was as it follows.

1. **Total velocity increment usage**
   Solve the Lambert's problem for 10 maneuvers to be done in two phases: from high orbit to low orbit, from low orbit to terminal orbit. Simulate them and compute the velocity increments. Evaluate the results.

2. **Lading conducive conditions map**
   Execute 372 simulations, scanning angular and radial position of an equatorial orbit. Evaluate the altitude value to check if in less than 50.000 s there was a landing, and, if yes, classify the initial condition as an LCC. If there was a landing, compute the final velocity with respect to the surface.

3. **Approximation maneuver and landing from an LCC**
   Calculate a maneuver so a vehicle begins in a high orbit, moves to a low orbit, then moves to a terminal orbit that has in it an LCC. Adjust the simulation so that, when the spacecraft reaches the LCC, the orbit is circular and the trajectory control is turned off. Execute the simulation and verify the landing.

4. RESULTS AND DISCUSSION

This section will show the results of the studies made according to the presented methodology. Fist for the asteroid (8567) 1996 HW1, later for the (1580) Betulia, the results to be presented will be: velocity increment usage in approximation maneuvers, the LCC mapping, and the use cases of the LCC maps combined with the approximation maneuvers.

4.1 Asteroid (8567) 1996 HW1 results

4.1.1 Total velocity increment usage

A set of 10 maneuvers was simulated. The initial conditions of the high and the final conditions of the terminal target orbits were fixed, while, at each maneuver, the target low orbits sizes were changed. The higher the number of the maneuver, the higher was the low orbit semimajor axis. The high initial orbit had a 32.250 m semimajor axis, initial true anomaly of 0 degree and other keplerian elements were zero. The final terminal target orbit had a semimajor axis of 3.000 m, final true anomaly of 360 degrees and other keplerian elements were zero. Low orbits had their semimajor axis varying from 3.900 m to 10.200 m, by 700 m increments, while having initial true anomalies of 180 degrees and other keplerian elements were zero. This information was used to solve the Lambert's problem for each maneuver, that were simulated with the STRS. Figure 4 shows the results.

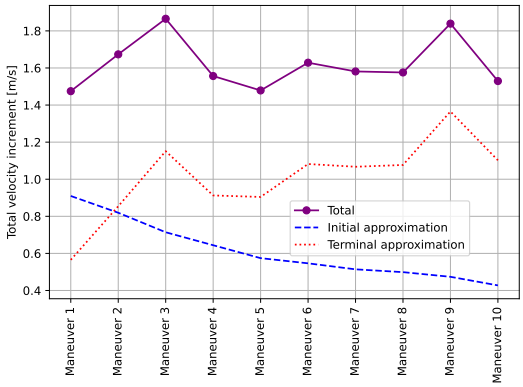

Figure 4. Total velocity increments computed for the approximation maneuvers around (8567) 1996 HW1.

Three kinds of information can be obtained from Figure 4: the total velocity increment for the whole maneuvers, the total velocity increment for the initial approximation and the total velocity increment for the terminal approximation. Regarding the initial approximation, the lower the low target orbit is, the higher is the velocity increment usage. Such a behavior cannot be identified in the terminal approximation line, which has a bigger variation and does not show a regular behavior. The 3 maneuvers with less velocity increment usage are 1, 5 and 10. The greater usage of velocity increments was on maneuvers 3 and 9.

4.1.2 Landing conducive conditions map

To map the LCC, a set of 372 simulations was made, respecting the definition of LCC presented previously. In the beginning of each simulation, BCI and BCBF coordinate systems were aligned, the initial orbit was circular, and it was varied the radial position vector magnitude and the initial angular position to the asteroid. Figure 5 shows the results of this simulations, making evident what initial condition was or was not an LCC.

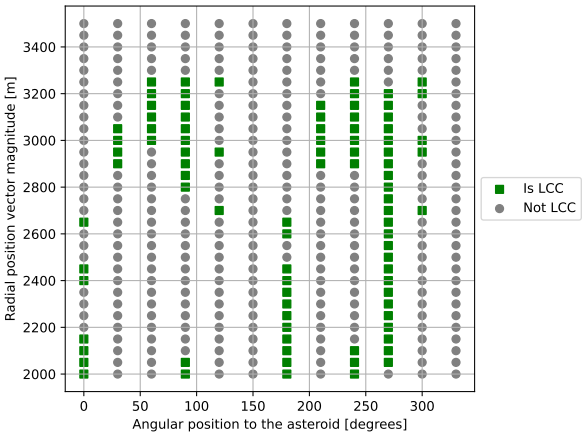

Figure 5. LCC map for (8567) 1996 HW1.

This result could be valuable for asteroid landing mission planning, because it could provide a reduction on velocity increment usage for deep space missions. To better explain this idea, let the following be considered. A spacecraft is in a circular high orbit of an asteroid. It must go to a low, then to a terminal orbit, from where it could land. In order to do that, the vehicle moves from the high orbit through a transfer orbit. Two transfer orbits drive the vehicle to the low and then to the terminal orbit, where the vehicle uses its propulsion system to adjust the orbital velocity and keep itself in a circular terminal orbit. From now, how could the spacecraft land? The trivial case would be to reduce the orbital velocity to zero, so it would fall vertically under the effect of the gravitational field. Another way to land would be by using the LCC map, which states: if the vehicle is in a radial and angular position that is an LCC, and if the orbit of the vehicle when it is in this position is circular, the vehicle will land in less than 50.000 s, because of the gravitational perturbations of the asteroid. But the vehicle was already in a circular orbit when it reached the terminal orbit, so it would not be needed another velocity increment in order for it to land. Hence, there would be the economy of the velocity increment that would be spent on the trivial case. Also, as an additional fact, none of the LCC points had produced final landing velocities, with respect to the asteroid surface, greater than 3,0 m/s, which was checked at the end of each simulation.

4.1.3 Use case of an approximation maneuver and landing from an LCC

A complete simulation of approximation and landing maneuver was made and is presented on Figure 6. In the left plot, the red line is the trajectory represented on BCI coordinates, and the blue line is the the trajectory represented in BCBF coordinates. The central asteroid shall be ignored when analyzing the BCI trajectory, while it has to be considered in the analysis of the BCBF trajectory. The upper right plot shows the three BCI axes of the velocity with respect to the surface. The lower right plot shows the altitude.

The BCI trajectory makes it clear the initial approximation, the terminal approximation, the hovering around the asteroid and the landing after reaching the LCC. This LCC is the one represented by a radial position magnitude of 2.900 m and angular position to the asteroid of 90 degrees, and it can be found by analyzing the BCBF trajectory. At the moment the LCC was reached, a velocity increment to circularize the orbit was applied and, as foreseen by the LCC map, the vehicle has landed in less than 50.000 s with a final velocity lesser than 3 m/s, which was verified in the simulation data. This result demonstrates the usability of the approximation and landing procedure presented previously and of the LCC map. The velocity plot shows the final velocity increment. The altitude plot shows the landing.

4.2 Asteroid (1580) Betulia results

4.2.1 Total velocity increment usage

A set of 10 simulations was made in order to allow the evaluation of the velocity increment usage around (1580) Betulia. The same maneuvering concept was used to bring the vehicle from a initial equatorial high circular orbit, with a semimajor axis of 90.855 m, to a target circular low orbit, and then from the low orbit to a target circular terminal orbit, with a semimajor axis of 4.400 m. The low orbits were scanned: the initial semimajor axis was 6.200 m and the final was 24.200 m, the increments of semimajor axis were of 2.000 m. The higher the number of the maneuver, the higher was the semimajor axis of the low orbit. Figure 7 shows the results.

Figure 7 shows a similar result if compared to what was shown for (8567) 1996 HW1. The initial approximation is approximately linear, in a sense that the smaller the semimajor axis of the low orbit, the greater the velocity increment usage. For the terminal approximation it does not happen, the behavior seen in the plot varies. For the terminal approxi-

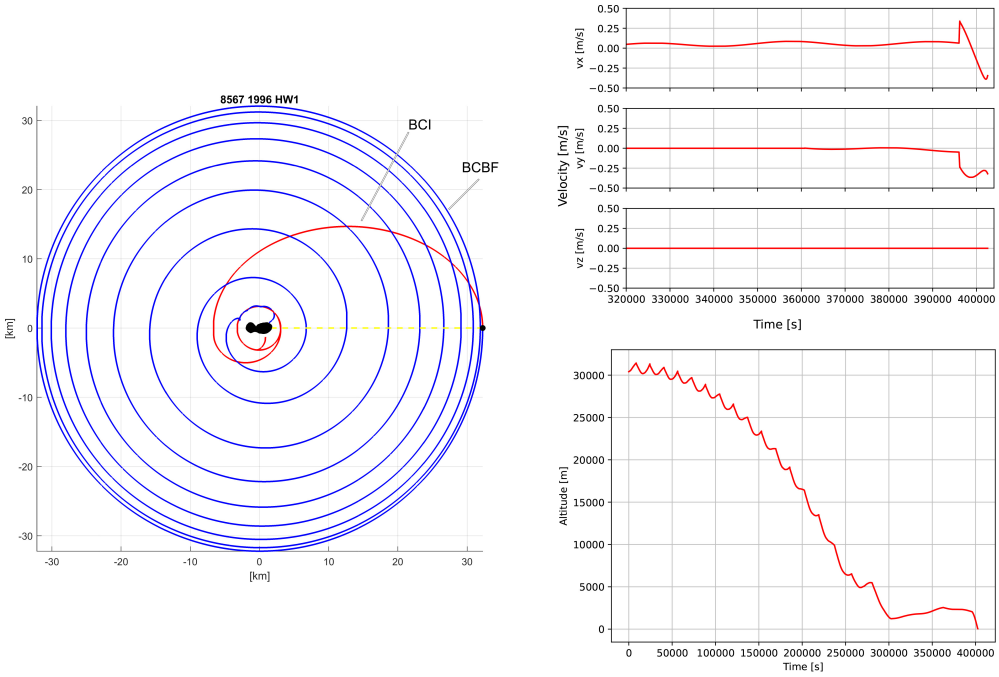

Figure 6. Left plot: simulation of a complete approximation and landing maneuver on (8567) 1996 HW1. The plot shows trajectories on BCI coordinates (red line) and on BCBF coordinates (blue line). Upper right: velocities with respect to the asteroid surface. Lower right: altitude plot, showing the landing in the end of the simulation.

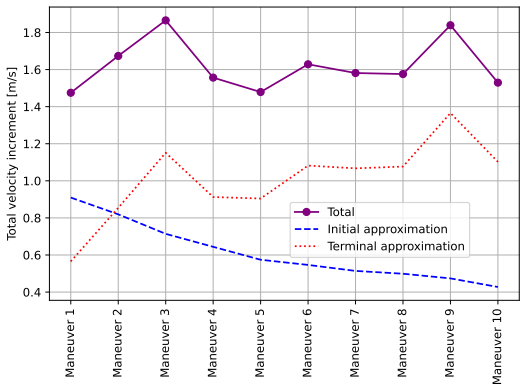

Figure 7. Total velocity increments computed for the approximation maneuvers around (1580) Betulia.

mation it can be said that the greater the trajectory from low to terminal orbit, the greater the time the vehicle is kept in a more disturbed region around the asteroid, so there is a tendency to a bigger velocity increment usage. Similarly to (8567) 1996 HW1, the maneuver that spent less velocity increments were 1, 5 and 10, while the greater velocity increments usage values happened on maneuvers 3 and 9.

4.2.2 Landing conducive conditions map

In order to investigate the existence of LCC on (1580) Betulia, the same procedure applied to (8567) 1996 HW1 was used. Figure 8 shows the results.

What can be seen is that (1580) Betulia also have LCC, as the map shows. Interestingly, the LCC occupies approximately the same regions in both asteroids. Since (1580) Betulia is more regular than (8567) 1996 HW1, it would be licit to assume that LCC maps could be found for other asteroids, specially if they have intermediate regularity (between the asteroids studied here). It also would make sense to suppose that asteroids more irregular than (8567) 1886 HW1, being more disturbed, would have LCC maps. This observations provide a direction for future researches regarding this theme.

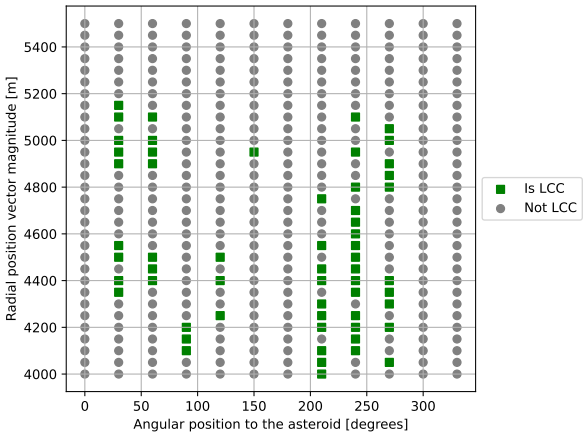

Figure 8. LCC map for (1580) Betulia.

4.2.3 Use case of an approximation maneuver and landing from an LCC

On Figure 9, the left plot shows the simulation for approximation and landing on (1580) Betulia, zoomed for better observation. The red trajectory is the movement represented on BCI coordinates, for which the plotted asteroid has to be ignored, and the blue trajectory is the BCBF one, for which the asteroid has to be considered. It can be seen in the BCBF trajectory that the LCC was reached around a radial position of approximately 4.900 m and an angular position relative to the asteroid of approximately 60 degrees, from which the land happened. The upper right plot shows the final moments of the velocity with respect to the surface. The lower right plot presents the altitude results, showing the landing at the end of the simulation.

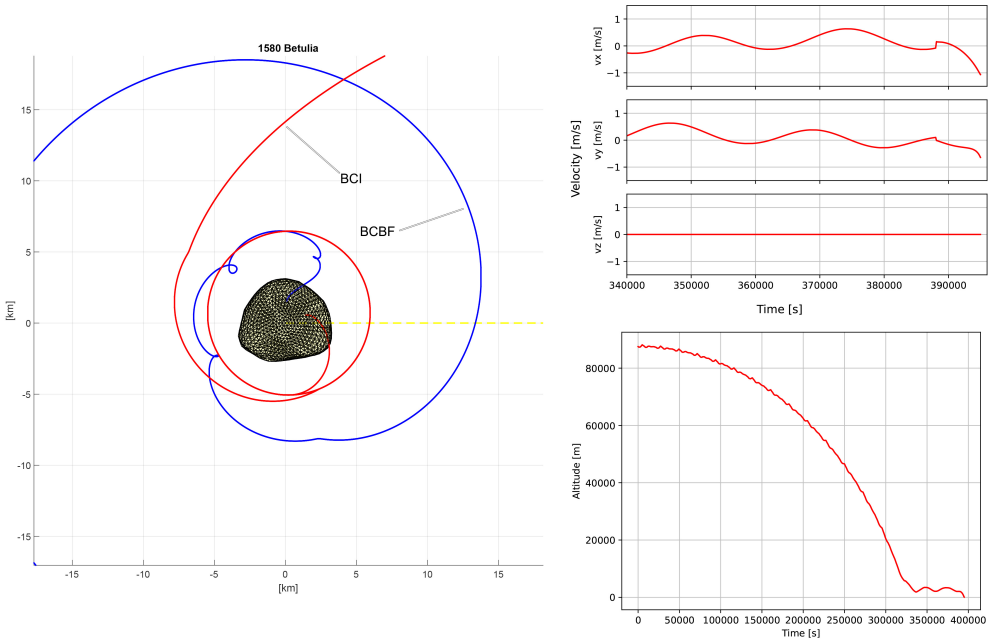

Figure 9. Left plot: simulation of a complete approximation and landing maneuver on (1580) Betulia, highlighting the landing. The plot shows trajectories on BCI coordinates (red line) and on BCBF coordinates (blue line). Upper right: velocities with respect to the asteroid surface. Lower right: altitude plot, showing the landing in the end of the simulation.

This subsection showed an application of the LCC map to an approximation and landing maneuver on (1580) Betulia. This results indicate the procedure made for (8567) 1996 HW1 have some degree of generality and can be reproduced and used for maneuvers around other asteroids. This results corroborates the value of the LCC map for planning space missions.

5. CONCLUSIONS

In this study, approximation and landing maneuvers were examined for the asteroids (8567) 1996 HW1 and (1580) Betulia. The research successfully improved our understanding of velocity increment usage. Additionally, the study revealed the existence of LCC maps for both asteroids and showed their use through approximation and landing maneuver simulations. A procedure was proposed for utilizing the LCC maps combined with approximation maneuvers, which usage was demonstrated through simulations. The usage of the LCC maps suggested that this tool could lead to advantages in asteroid missions by reducing the required total velocity increment. Furthermore, based on the LCC map results, it can be inferred that asteroids with intermediate regularity in their gravitational fields, lying between (8567) 1996 HW1 and (1580) Betulia, much likely possess LCC maps as well. This insight shows the direction of future research.

6. ACKNOWLEDGEMENTS

We thank CAPES for deeply supporting this research financially. Also, we thank INPE for providing an amazing structure so we could produce this work. And we thank for the laboratory colleagues, with whom good talks enlightened our understanding and helped with some tricky algorithm problems.

7. REFERENCES

Battin, R., 1999. *An Introduction to the Mathematics and Methods of Astrodynamics*. AIAA education series. American Institute of Aeronautics and Astronautics.

Beshore, E., Lauretta, D., Boynton, W., Shinohara, C., Sutter, B., Everett, D., Gal-Edd, J., Mink, R., Moreau, M. and Dworkin, J., 2015. "The osiris-rex asteroid sample return mission". *2015 IEEE Aerospace Conference*, pp. 1–14.

Clark, B.E., Barucci, M.A., Zou, X.D., Fulchignoni, M., Rivkin, A., Raymond, C., Yoshikawa, M., Elkins-Tanton, L.T. and Levison, H., 2018. "Chapter 1 - a brief history of spacecraft missions to asteroids and protoplanets". In N. Abreu, ed., *Primitive Meteorites and Asteroids*, Elsevier, pp. 1–57.

Daly, R.T., Ernst, C.M., Barnouin, O.S., Chabot, N.L., Rivkin, A.S., Cheng, A.F., Adams, E.Y., Agrusa, H.F., Abel, E.D., Alford, A.L. *et al.*, 2023. "Successful kinetic impact into an asteroid for planetary defense". *Nature*, pp. 1–3.

Fernandes, S.S. and de Paula Santos Zanardi, M.C.F., 2018. *Fundamentos de astronáutica e suas aplicações*, Vol. 1 of *Aerospace Engineering*. Editora da Universidade Federal do ABC, 1st edition.

Frieger, G., 2021. "3d asteroide catalog". https://3d-asteroids.space/asteroids. Accessed 28 Jan 2023.

Hashimoto, T., Kubota, T., Kawaguchi, J., Uo, M., Shirakawa, K., Kominato, T. and Morita, H., 2010. "Vision-based guidance, navigation, and control of hayabusa spacecraft - lessons learned from real operation -". *IFAC Proceedings Volumes*, Vol. 43, No. 15, pp. 259–264. 18th IFAC Symposium on Automatic Control in Aerospace.

Mingtao, L. and Kaiduo, W., 2022. "Progress of planetary defense research in china". *Chinese Journal of Space Science*.

Mitchell, R.T., 2000. "The cassini/huyegens mission to saturn and titan".

Mota, M.L., 2017. *Modelo do campo gravitacional de um corpo com distribuição de massa irregular utilizando o método da expansão do potencial em série e determinação de seus coeficientes dos harmônicos esféricos*. Ph.D. thesis, Instituto Nacional de Pesquisas Espaciais (INPE), São José dos Campos.

Ogata, K., 1997. *Engenharia de controle moderno*. Pearson Prentice Hall, 3rd edition.

Rocco, E.M., 2008. "Analysis of the deviations of the trajectory due to the terrestrial albedo applied to some scientific missions". In *Proceedings of the International Conference on Mathematical Problems in Engineering, Aerospace and Sciences*. Genova, Italy.

Rocco, E.M., 2013a. "Simulação de manobras orbitais impulsivas com empuxo limitado e controle de trajetória em malha fechada". In *Proceeding Series of the Brazilian Societyof Applied and Computational Mathematics*. Vol. 1.

Rocco, E., 2010. "Evaluation of the terrestrial albedo applied to some scientific missions". *Space Science Reviews*, Vol. 151, pp. 135–147.

Rocco, E., 2013b. "Automatic correction of orbital elements using continuous thrust controlled in closed loop". *VII Congresso Nacional de Engenharia Mecânica*.

Rocco, E., 2015. "Gravitational disturbances generated by the sun, phobos and deimos in orbital maneuvers around mars with automatic correction of the semi-major axis". *Journal of Physics: Conference Series*, Vol. 641, p. 012027.

Taylor, M.G.G.T., Altobelli, N., Buratti, B.J. and Choukroun, M., 2017. "The rosetta mission orbiter science overview: the comet phase". *Philosophical Transactions of the Royal Society A: Mathematical, Physical and Engineering Sciences*, Vol. 375, No. 2097, p. 20160262.

Veverka, J., Belton, M., Klaasen, K. and Chapman, C., 1994. "Galileo's encounter with 951 gaspra: Overview". *Icarus*, Vol. 107, No. 1, pp. 2–17.

8. RESPONSIBILITY NOTICE

The authors are solely responsible for the printed material included in this paper.